Check for updates

Propellants, Explosives, Pyrotechnics

WILEY-VCH

Propellants, Explosives, Pyrotechnics

RESEARCH ARTICLE OPEN ACCESS

Factorial Analysis of the Influence of Both Water and Oxygen on Extruded Double Base Rocket Propellant Decomposition

Alonso Romero Jabalquinto[1] | Nathalie Mai[1] | Moritz Heil[2] | Guillermo Frades Castedo[3] | Philip P. Gill[1,4]

[1]Cranfield University, Defence Academy of the United Kingdom, Shrivenham, Swindon, UK | [2]Fraunhofer-Institut für Chemische Technologie ICT, Pfinztal, Germany | [3]Universidad Del Valle de Mexico, Santiago de Querétaro, Queretaro, Mexico | [4]Roxel Ltd, Summerfield Lane, Kidderminster, United Kingdom

Correspondence: Nathalie Mai (n.mai@cranfield.ac.uk)

Keywords: chemical stability | extruded double base rocket propellant | Friedman differential isoconversional method | heat flow calorimetry | oxygen | water

ABSTRACT

The decomposition mechanisms of double base rocket propellants are well known and reported, but the influence of atmospheric conditions such as water and oxygen is poorly understood. In this work, the influence of water and oxygen on an extruded double base (EDB) rocket propellant aged between 70 and 100°C was examined using heat flow calorimetry. The results show that increased water content and higher oxygen concentration both lead to elevated heat flow. The activation energy (E_a), which was determined using the Friedman differential isoconversional method, showed that Ea decreases with higher water content, suggesting water acts as a catalyst, while lower oxygen concentration increases Ea, indicating slower decomposition. Factorial design analysis confirmed that both factors negatively impact E_a, with oxygen being the more significant factor while the water/oxygen interaction (AB) on the E_a is negligible. This research provides critical insight into the factors affecting the stability and shelf life of rocket propellants, which can lead to improved formulations and storage conditions, augmenting the safety and performance of EDB rocket propulsion systems. This research provides critical insight into the factors affecting the stability and shelf life of rocket propellants, which can lead to improved formulations and storage conditions, augmenting the safety and performance of EDB rocket propulsion systems.

1 | Introduction

Since the 1940s, most tactical rockets have been sealed to avoid contact with water and oxygen in the atmosphere [1]. Studies conducted in the 1970s revealed that propellants contained in rockets with faulty seals performed poorly owing to moisture and oxygen exposure [2]. However, they did not go into detail on how these factors affected the chemical decomposition of double base (DB) propellants.

The nitrate esters (nitrocellulose [NC] and nitroglycerin) decomposition process for DB rocket propellant begins with the O-NO_2 bond homolytic cleavage. This leads to the release of nitrogen oxides (NO_x) [3, 4]. There are two known mechanisms for this process, hydrolysis (Equations (1) and (2)) and thermolysis (Equation (3)) [5].

$$R-O-NO_2 + H_2O \xrightarrow{H+} R-OH + HNO_3 \quad (1)$$

$$R-OH + HNO_3 \rightarrow R-CHO + NO_2 + H_2O \quad (2)$$

$$R-O-NO_2 \rightarrow RO^{\cdot} + NO_2 \quad (3)$$

The presence of water in the propellant enables the hydrolytic splitting of the O-NO_2 bond in the nitrate esters. The released

Abbreviations: 2-NDPA, 2-nitro-diphenylamine; DB, double base; DSC, differential scanning calorimetry; DTA, differential thermal analysis; EDB, extruded double base; GC-MS, gas chromatography-mass spectrometry; HF, heat flow; HFC, heat flow calorimetry; NC, nitrocellulose; NO_x, nitrogen oxides; RH, relative humidity; TGA, thermogravimetric analysis.

This is an open access article under the terms of the Creative Commons Attribution License, which permits use, distribution and reproduction in any medium, provided the original work is properly cited.

© 2025 The Author(s). *Propellants, Explosives, Pyrotechnics* published by Wiley-VCH GmbH.

NO_x radicals react with the water forming HNO_3, which further accelerates the decomposition process [6]. It should be noted that, at the standard storage temperature of these energetic materials (25°C), hydrolysis is the dominant mechanism [7, 8]. As the temperature increases, the rate of decomposition by hydrolysis also increases; however, at approximately 60°C, thermolysis becomes the predominant mechanism of decomposition. According to O'Keefe et al. [9], the presence of water does not affect the thermolysis decomposition kinetics.

Guillaume et al. [10] analysed the heat flow (HF) evolution in DB ball propellant samples with different (0%–65%) relative humidities (RHs) at 80°C by HF calorimetry (HFC). They demonstrated that increasing the RH can increase HF by up to 30%. Eerlingh et al. [11] discussed the RH influence on the ageing of single base propellants at 85°C using HFC. Their results showed that moisture added (75% RH) to the samples increased the HF by 300% compared to samples with low RH. Similarly, Jabalquinto et al. [12] reported that the presence of water significantly affects the EDB rocket propellant decomposition process using HFC. They observed that high moisture concentrations (95% RH) in these energetic formulations might enhance HF by up to 400% (from 35 to 143 μW/g), resulting in a loss in shelf life.

Oxygen plays an important role in the decomposition chemistry of NC and DB propellants. Lurie et al. [13], reported that oxygen enhances self-acceleration in the NC thermal decomposition. This phenomenon is due to O_2 oxidising NO to the more reactive NO_2. Although oxygen is generally a much weaker oxidant than NO_2, in the presence of NO_2 it can actively participate in redox transformations through a peroxide mechanism associated with alkyl radicals [14]. The above is illustrated in the following equations:

$$R - O - NO_2 \rightarrow R - O^{\cdot} + NO_2^{\cdot} \quad (4)$$

$$R - H + NO_2^{\cdot} \rightarrow R^{\cdot} + HNO_2 \quad (5)$$

$$R^{\cdot} + O_2 \rightarrow R - O - O^{\cdot} \quad (6)$$

$$R - O - O^{\cdot} + NO_2 \rightarrow R - O^{\cdot} + NO_2^{\cdot} \quad (7)$$

$$R - O - O^{\cdot} + R - H \rightarrow R^{\cdot} + R - O - OH^{\cdot} \quad (8)$$

Li et al. [15] assessed the thermal hazard of NC solutions in varying oxygen levels (0%–21% v/v O_2) using thermogravimetric analysis (TGA) and differential scanning calorimetry (DSC). They found that removing all oxygen increased the activation energy of thermal decomposition by up to 32% (from 166 to 220 kJ/mol), showing that oxygen significantly affects NC thermal decomposition. Furthermore, Katoh et al. [16] studied the spontaneous ignition mechanism of NC isothermally stored at 77°C in atmospheres with different O_2 concentrations using HFC. According to their observations, the induction time for autoignition dropped by 66%, from 10 to 3.4 h, as the O_2 content increased from 0% to 21%. Guillaume et al. [10] used HFC to analyse HF evolution at 80°C in DB-ball propellants with the air removed from the vials, showing that the removal of oxygen reduced the overall HF production by up to 30% compared to samples with air.

Heemskerk and van de Mey [17] evaluated the thermal stability of single-base gun propellants under different levels of water content (0%, 1%, and 2.4% w) and O_2 (0%, 5%, 10%, and 20% v/v O_2) concentrations at 77°C using HFC. Their research found that both factors influence thermal stability, and 100% RH at 25°C and 21% v/v O_2 increases HF by 50% compared to samples with low moisture content and no oxygen. However, they did not determine which factor is more significant in the decomposition of NC-based propellants, only indicating that moisture content and increased O_2 concentration stimulate this process.

In summary, while the hydrolysis of DB rocket propellant requires water, thermolysis does not. Although oxygen plays a role in thermolysis, there is no evidence in the literature that oxygen is involved in hydrolysis.

Thermal analysis techniques are used for process safety, chemical stability and compatibility across a range of industries, such as i) pharmaceutical industry to assess drug stability and compatibility, ii) metallurgy to measure metal corrosion rates, iii) construction industry to determine cement curing times, and iv) to evaluate the shelf life of energetic materials. [18–21]. Classical thermo-analytical micro methods (differential thermal analysis [DTA] and DSC) are still very useful, but medium-scale instruments based on HF measurement are becoming increasingly important [22].

Reaction calorimetry methods such as HFC measure heat generated by chemical reactions at a constant temperature over time. It provides sensitive results, detecting even small changes in heat production (order of microwatt—μW), such as slow decomposition in nitrate esters base propellants stored at room temperature [23]. Unlike other accelerated ageing tests, such as stabiliser consumption, the HFC is a global method as it considers all physicochemical changes that produce heat [24, 25]. The shape of the generated HF curve, in this case for a 2-nitro-diphenylamine (2-NDPA) stabilised EDB rocket propellant, is directly influenced by the chemical reactions as described in Figure 1.

The data obtained from a minimum of three different HFC temperatures can be used to calculate the kinetic parameters [26], such as the activation energy (E_a), the pre-exponential factor (A), and the reaction mechanism function (f(α)) [27].

For the determination of the kinetic parameters, isoconversional methods are used, which are based on the principle that for a constant degree of conversion (α), the reaction rate is only a function of temperature [28]. There are different isoconversional methods such as the Ozawa-Flynn-Wall and the Vyazovkin integration method, however, the Friedman differential model is the most suitable for determining the kinetic parameters due to the isothermal nature of the HFC test [29, 30].

Based on the Arrhenius equation, Friedman [31] proposed to use it to determine E_a, A and f(a) from its linearization, expressing itself as follows:

$$\ln\left(\frac{d\alpha}{dt}\right) = -\frac{E_a}{RT} + \ln\left[Af(\alpha)\right] \quad (9)$$

where $(\frac{d\alpha}{dt})$ is the reaction rate, R is the gas constant (8.314 J/mol K), E_a is the activation energy (kJ/mol), and T is the temperature (K).

15214087, 0, Downloaded from https://onlinelibrary.wiley.com/doi/10.1002/prep.12070 by Cranfield University Kings, Wiley Online Library on [10/06/2025]. See the Terms and Conditions (https://onlinelibrary.wiley.com/terms-and-conditions) on Wiley Online Library for rules of use; OA articles are governed by the applicable Creative Commons License

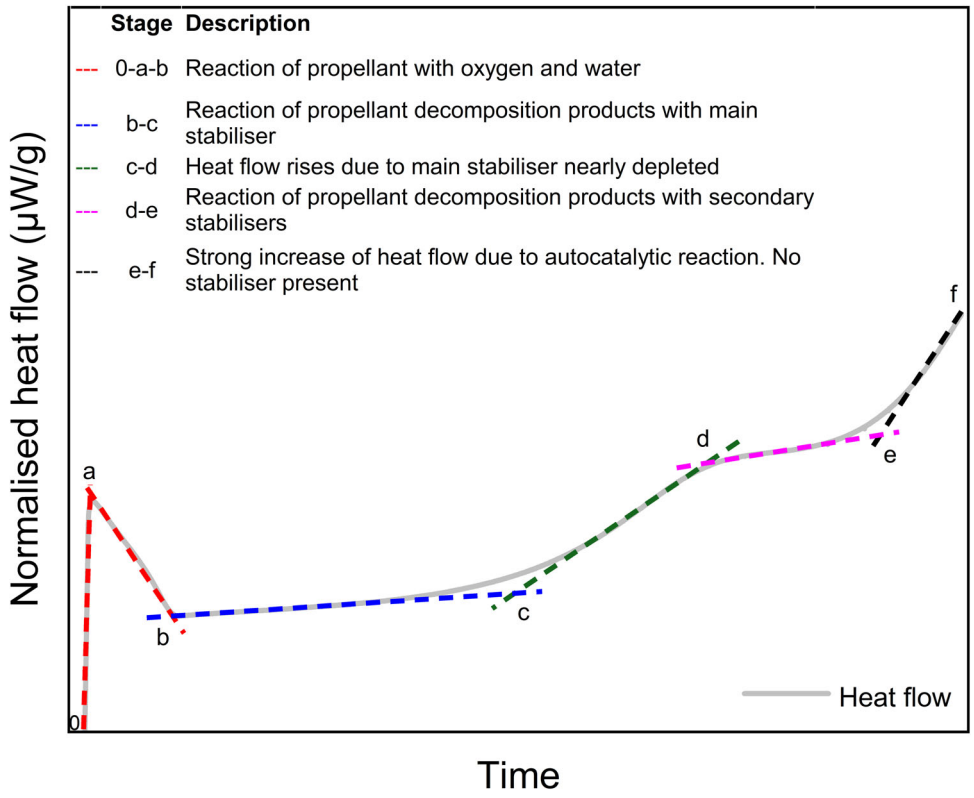

FIGURE 1 | Heat flow evolution in a double base (DB) rocket propellant. The dotted lines are a linearization of the different stages of decomposition of a nitrocellulose (NC)-based propellant identified in the heat flow calorimeter (HFC). Reprinted [12] with permission from Creative Commons CC-BY license.

Friedman differential isoconversion method has advantages such as i) no assumptions on reaction mechanism required and ii) less dependence on the choice of the degree of conversion [32]. The conversion (α) represents an experimentally determined parameter as a function of the change of a physical or chemical property. In the case of HFC, it is the generated heat, which describes the process under study. The conversion is determined as follows [4, 33]:

$$\alpha = \frac{Q_t - Q_i}{Q_{end} - Q_i} \tag{10}$$

where Q_t, Q_i, and Q_{end} (J/g) represent the heat at time t (s), t = 0 (experiment starts) and t = t_{end} (experiment ends), respectively.

Substituting Equation (10) into Equation (9), the kinetic parameters can be determined from the HFC data [34]:

$$\ln\left(\frac{d\alpha}{dt}\right) = \ln\left(\frac{HF_t}{Q_{end} - Q_i}\right) = -\frac{E_a}{RT} + \ln\left[A \cdot f(\alpha)\right] \tag{11}$$

where HF_t (µW/g) is the heat flow at a specific time (t).

The simultaneous effects of both oxygen and water on the chemical decomposition of DB propellants have not been extensively discussed in the literature. The aim of this work is to assess the effect of oxygen and water content on the decomposition chemistry of EDB rocket propellants and their implications on their shelf life. EDB propellant samples have been artificially aged at 70, 80, 90, and 100°C, with varying water content (ranging from 0.8 to 4 µL/g) and different oxygen content (1% and 21% v/v). The kinetic parameters of propellant decomposition under the action of the above factors were determined by the Friedman differential isoconversional method.

2 | Material and Methods

The propellant used was an extruded double base (EDB) rocket propellant billet (ø40 mm × 38 mm) consisting of NC 5%–57% w/w, nitro-glycerine 19%–46% w/w, 2 nitro-diphenylamine 1%–8% w/w, and copper oxide 0%–3% w/w/, which was cut and sieved to 3 mm particles [35]. These particles were then placed into 3 cm^3 HFC crimp seal glass ampoules with a propellant loading density of 0.80 g/cm^3 (e.g. 2.4 g in 3 cm^3 vial). All samples were dried in a vacuum desiccator for 48 h.

Under an argon-rich atmosphere or air, water was added to the vials in volumes of 2, 4, 7, and 10 µL (using a 20 µL micropipette), resulting in normalised water contents of 0, 0.8, 1.6, 2.8, and 4.0 µL/g, respectively, before crimping the ampoules. Water content is reported as absolute humidity in µL/g (Using RH% would be misleading because of the different temperaturestested). The oxygen concentration in the samples was measured by headspace gas chromatography-mass spectrometry (GC-MS). Table 1 displays the chromatographic conditions that were employed.

Using a TA Instruments TAM-IV microcalorimeter system, the HFC was measured isothermally at temperatures of 70, 80, 90, and 100°C for up to 45, 15, 7, and 3 days, respectively. The calorimeter

15214087, 0, Downloaded from https://onlinelibrary.wiley.com/doi/10.1002/prep.12070 by Cranfield University Kings, Wiley Online Library on [10/06/2025]. See the Terms and Conditions (https://onlinelibrary.wiley.com/terms-and-conditions) on Wiley Online Library for rules of use; OA articles are governed by the applicable Creative Commons License

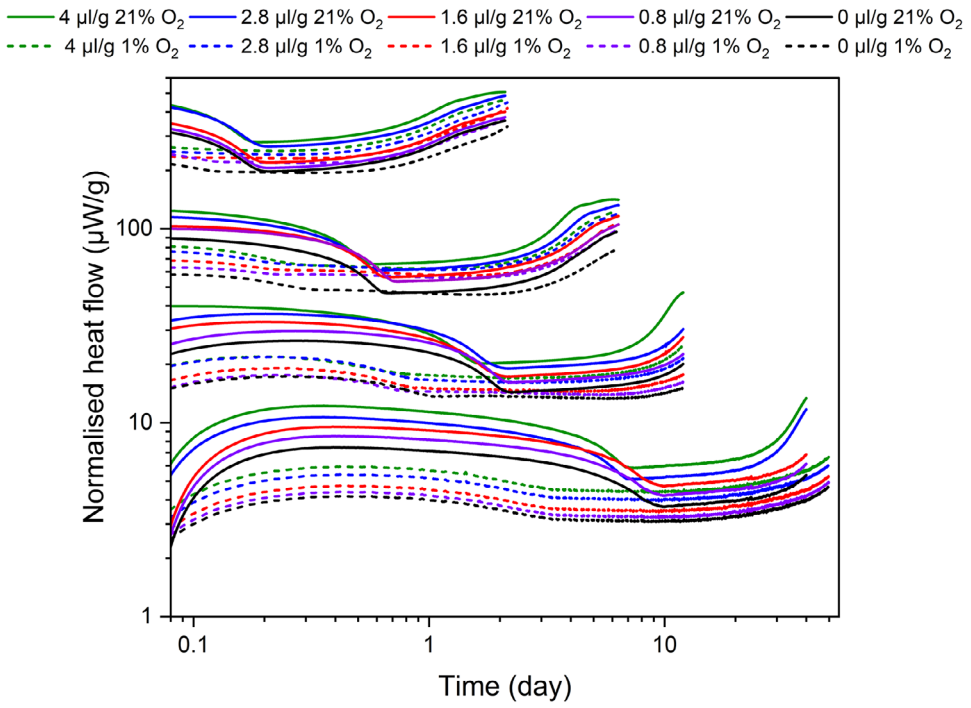

FIGURE 2 | Log/log plot showing the influence of water and oxygen on normalised average heat flow of extruded double base (EDB) rocket propellant at different temperatures. The straight solid lines shown in the graph are the heat flow generated by the samples with an oxygen concentration of 21% volume/volume, whilst the samples with 1% oxygen are shown with dotted lines.

TABLE 1 | Gas-chromatography-mass spectrometry (GC-MS) conditions for oxygen concentration analysis.

Gas chromatographer	**Aligent Technologies 7890 B**
Mass spectrometer detector	Aligent Technologies 5977 AMSD
Column	Aligent Technologies PoraPlotQ 25 mm × 0.25 mm film diameter (DF) = 8.0 µm
Flow rate	1.2 mL/min
Temperature range	30°C–250°C
Inlet temperature	220°C
MSD transfer line	200°C
Split ratio	50
Injection	250 µL
Replicates	2 per sample

was calibrated at each temperature, and the baseline was recorded before and after the test. Each test was performed in duplicate.

3 | Results and Discussion

3.1 | HFC Results

The average HF from EDB rocket propellant samples with different oxygen concentrations and water volumes are shown in Figure 2. It is observed that both water and oxygen influence HF. At all temperatures assessed, increasing water content results in higher HF. This is evident as samples with 4 µL/g water content produce the highest HF. As for the oxygen concentration, as the O_2 concentration decreases, the HF also decreases. Specifically, samples with 0 µL/g water content and 1% O_2 concentration have the lowest HF at all temperatures tested.

Changes in O_2 concentration cause variations in the shape of the generated HF curve, as shown in Figure 3. The initial peak maximum was previously defined as "a" (Figure 1) and the overall HF is reduced by up to 35% when oxygen concentration decreased from 21 to 1%. This initial exothermic reaction is reported to be due to $NO^{\bullet}$ radicals reacting with oxygen to release NO_2 [10, 25]. In addition, the inflexion point "b" occurs sooner in the low O_2 concentration samples, hence HF difference between points "a" and "b" is three times greater in samples containing 21% v/v O_2 compared to those with 1% v/v O_2.

3.2 | Kinetic Reaction Analysis

The Friedman differential method (Equation (3)) is used to determine the activation energy from the HF data, considering the effects of O_2 and water levels in the samples. In the literature [36], an arbitrary value of Q_{end} has been selected in order to calculate α (Equation (2)). However, the HF curve shape changes with time and test temperatures. This may result in some HF values being influenced by other reactions, which will change the E_a result. Therefore, in this study, 15J/g was chosen as the value for Q_{end}, as this value was within the main stabilising reaction (b-

15214087, 0, Downloaded from https://onlinelibrary.wiley.com/doi/10.1002/prep.12070 by Cranfield University Kings, Wiley Online Library on [10/06/2025]. See the Terms and Conditions (https://onlinelibrary.wiley.com/terms-and-conditions) on Wiley Online Library for rules of use; OA articles are governed by the applicable Creative Commons License

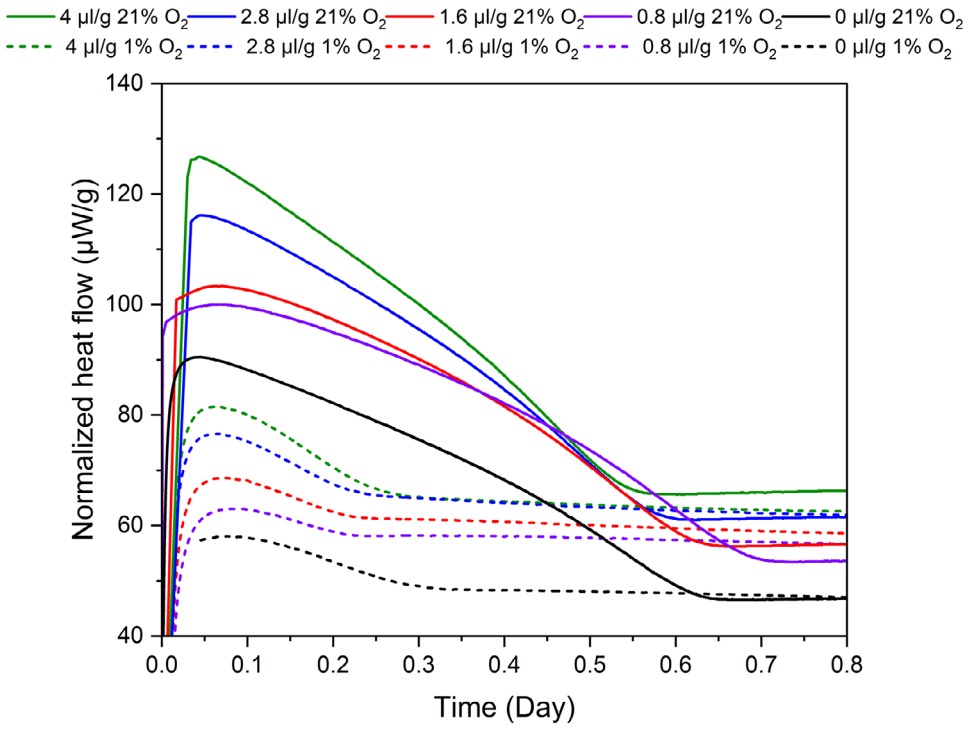

FIGURE 3 | Influence of water and oxygen on the normalised average heat flow of an extruded double base (EDB) propellant at 90°C. Data were extracted from Figure 2 and expanded to show heat flow over 0.8 days (axes are not in log/log for clarity).

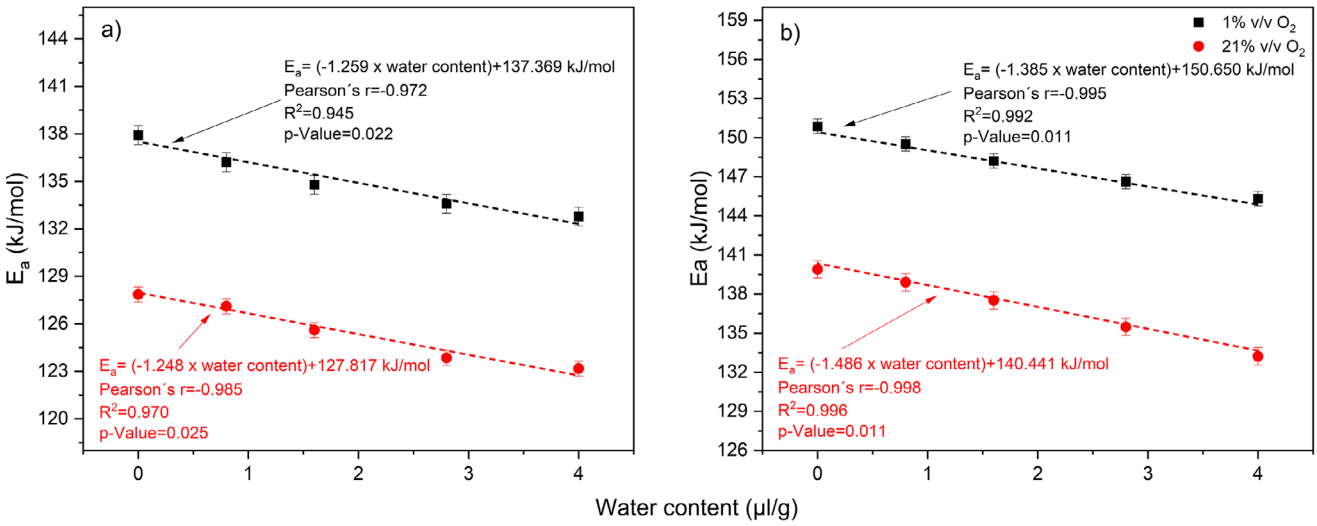

FIGURE 4 | Effect of water on the activation energy (E_a) linear regressions plotted for (a) region a-b and (b) region b-c. Isoconversional point 5 J/g was selected in region a-b and 15 J/g for region b-c.

c) for all conditions tested. The values used can be found in Table S1.

The results of the E_a in both regions are shown in Figure 4. In every case, the slopes of the linear regressions are negative, suggesting that, as water content increases, E_a consistently decreases in the regions of the HF curve studied. Likewise, the correlation coefficients (r) given by the Pearson test of the linear regressions indicated a strongly negative correlation ($r < -0.9$), which implies that the E_a variability can be explained by the water contained in the samples. Finally, the p-value obtained from the Pearson correlation test ($p < 0.05$) confirms a statistically significant relationship between water and E_a. Overall, these results suggest that water influences E_a by significantly reducing it with increasing concentration.

The activation energies reported in this work for samples with different amounts of water present in the region where the stabiliser reacts with NO_x (b-c) in a 21% v/v O_2 atmosphere, are consistent with previously presented results [12]. Samples with lower water concentration present a higher E_a (135 kJ/mol at 6 g/m^3 AH), whilst samples with higher amounts of water present

15214087, 0, Downloaded from https://onlinelibrary.wiley.com/doi/10.1002/prep.12070 by Cranfield University Kings, Wiley Online Library on [10/06/2025]. See the Terms and Conditions (https://onlinelibrary.wiley.com/terms-and-conditions) on Wiley Online Library for rules of use; OA articles are governed by the applicable Creative Commons License

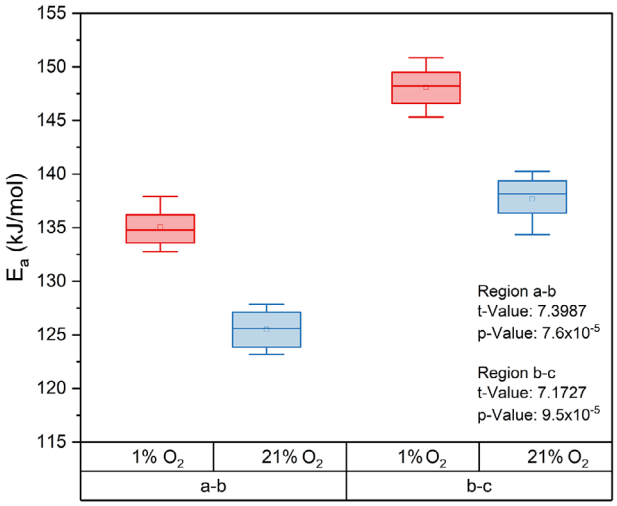

FIGURE 5 | Boxplots showing the activation energy (E_a) distribution for different oxygen concentration levels in the heat flow regions studied.

have a lower E_a (130 kJ/mol at 22 g/m^3 AH). However, for the region where O_2 reacts with the propellant DB (a-b), there are no E_a values reported in the literature to compare the results obtained.

Linear regression for the effect of O_2 cannot be done because only two concentrations of O_2 were used during this research, therefore boxplots of the E_a distribution of each O_2 concentration in the analysed regions of the HFC curve are presented in Figure 5. These boxplots showed that the E_a values for each 1% O_2 v/v concentration are higher than those for higher O_2 concentrations. The medians (horizontal line within the box) for the lower O_2 concentration are higher, suggesting that E_a decreases as O_2 concentration increases. The *t*-Value ($t > 7$) and p-value ($p < 0.05$) confirmed that O_2 significantly affects Ea. In summary, these results showed that at higher O_2 concentrations, E_a decreases significantly compared to lower O_2 concentrations.

Guillaume et al. [10] explain that the difference in E_a between samples with low and high O_2 concentrations is due to the increased availability of O_2. In samples with higher O_2 content, sufficient O_2 is present to oxidise the NO, produced by NC, to NO_2. The generated NO_2 then reacts with 2-NDPA, consuming it more rapidly. This exothermic reaction between NO_2 and the stabiliser explains the increase in HF [18].

The kinetic analysis performed using the Friedman differential method reveals that Ea is different in both O_2 concentrations across the four water concentrations assessed (Figure 5). These reported E_a, according to the literature [24, 25], are within the range stated for thermolysis as the dominant decomposition reaction, omitting hydrolysis as a decomposition mechanism. However, as previously demonstrated [9, 35], the water has no effect on the NC-based propellant thermolytic decomposition, implying that the observed mechanism is not hydrolysis, but more likely a catalytic reaction. This is observed at both O_2 concentrations tested.

Water and O_2 concentrations impact on EDB rocket propellant decomposition can be analysed by factorial design, as it is a useful statistical tool for understanding the joint effect of certain factors (water and O_2) and their interactions on a response (HF or E_a) [37, 38]. The effect of a factor can be defined as the observed change in the response variable due to the change in the level of the factor, this is determined as follows [39]:

$$Effect_{H_2O} = \frac{1}{m_{H_2O}} \sum_{i=1}^{m} \left(\mu_{E_a H_2O} - \mu_{E_a T} \right) \quad (12)$$

$$Effect_{O_2} = \frac{1}{n_{O_2}} \sum_{j=1}^{n} \left(\mu_{E_a O_2} - \mu_{E_a T} \right) \quad (13)$$

where m_{H_2O} is the number of water levels (0.8, 2.8, 1.6, and 4 µL/g), n_{O_2} is the number of oxygen levels (1% and 21% O_2 v/v), $\mu_{E_a H_2O}$ is the mean of the responses (HF or E_a) at a specific level of the water factor, $\mu_{E_a O_2}$ is the mean of the HF or E_a at a specific level of the oxygen factor, and $\mu_{E_a T}$ is the average of all HF and E_a.

Two factors have an interaction effect on the HF or E_a when the effect of one factor depends on the level at which the other factor is found. The interaction between the factors and the HF or E_a is determined as follows [39]:

$$Interaction_{H_2O,O_2} = \frac{1}{m_{H_2O} n_{O_2}} \sum_{i=1}^{m} \sum_{j=1}^{n} \left(\mu_{AiBj} - \mu_{E_a H_2O} - \mu_{E_a O_2} + \mu_{E_a T} \right) \quad (14)$$

where μ_{AiBj} is the mean of the E_a or HF for a specific combination of oxygen and water levels.

The factorial analysis makes use of various graphical tools in order to determine how the E_a or HF is influenced by the concentration of O_2 and water contained in the propellant samples. One of these tools is the response surface graph (Figure S1) which illustrates how the response, in this case the E_a, changes with variations in the concentration of O_2 and water across different samples. However, these plots do not show which of the factors and their interactions are the most significant in the E_a. Using Equations (12–14), a Pareto diagram can be plotted [39]. This diagram, along with the normal probability plot of standardised effects can be used to understand the importance of the effects and their interactions [40]. The Pareto diagram highlights the most significant effects in absolute terms but does not show how they influence the response, whilst a normal probability plot of standardized effects provides a comprehensive view of the direction and magnitude of the effects and interactions.

The Pareto diagrams in Figure 6a,b show that the E_a in both regions of the HFC curve is influenced by the oxygen (A) and water (B) concentrations, with oxygen concentration having a more pronounced effect. According to Evans and Gordon [2], the maximum RH under standard storage conditions (T = 25°C and 21% O_2 v/v) is above 95% RH. In this work, the maximum amount of water used (4 µL/g) is equivalent to 145% RH at 25°C. However, the RH cannot exceed 100% in practice, so the flask would be saturated, and the excess water would remain in liquid form at 25°C. The diagram also indicates that the water/oxygen interaction (AB) is very small, therefore it can be neglected.

15214087, 0, Downloaded from https://onlinelibrary.wiley.com/doi/10.1002/prep.12070 by Cranfield University Kings, Wiley Online Library on [10/06/2025]. See the Terms and Conditions (https://onlinelibrary.wiley.com/terms-and-conditions) on Wiley Online Library for rules of use; OA articles are governed by the applicable Creative Commons License

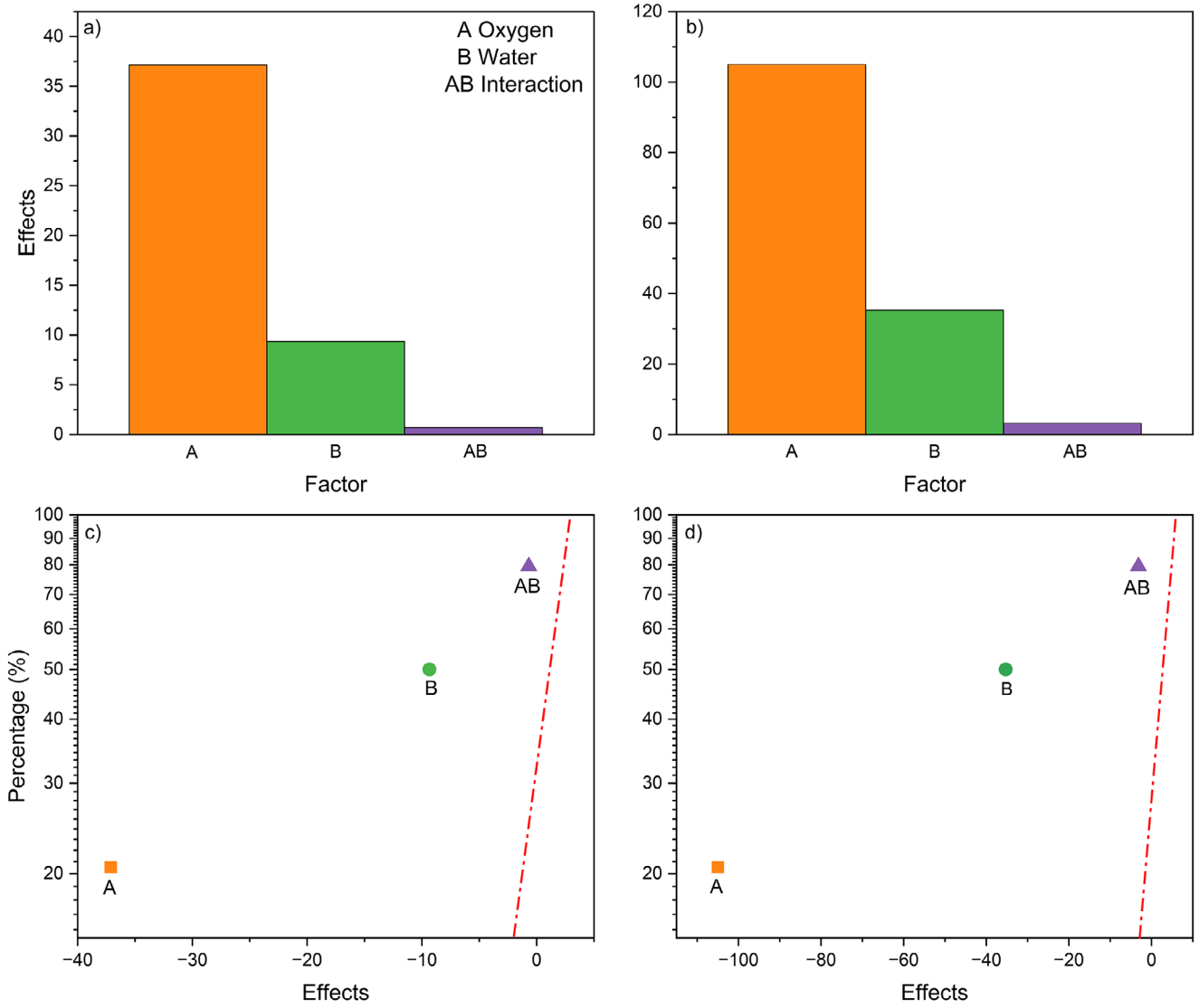

FIGURE 6 | Pareto (a and b) and normal probability plots (c and d) of the effects and interactions between the water contained and oxygen concentration on the activation energy (E_a). Plots a) and c) correspond to the results for the a-b region, while plots b) and d) correspond to the results for the b-c region. On the normal probability plot, the further the effects are from the normal distribution (red dash-dotted line) the more likely they will have a real impact on the E_a at a confidence level of 95%.

The normal probability plot of the effects in Figure 6c,d shows that O_2 concentration and water content are on the left side of the normal distribution line, indicating that as any of these effects increase, the E_a decreases. The water/oxygen interaction AB is very close to the normal distribution line indicating that it is not statistically significant and can therefore be discarded.

In Figure 4a,b, E_a decreases with more water, and the lines for different O_2 levels remain almost parallel. The O_2 concentration stays consistent across different water levels, and the effects of water are consistent across O_2 levels. There is no interaction between these effects, so they can be analysed individually.

According to Katoh et al. [14], oxygen has a more significant influence on NC decomposition than water. They observed that exothermic decomposition hardly occurs in an oxygen-free atmosphere, indicating that oxygen is a crucial factor for decomposition. Furthermore, they suggest that exothermic decomposition is caused by oxygen and enhanced by the presence of water. Although water also plays an important role in accelerating decomposition in oxygen atmospheres, they concluded that decomposition does not occur solely through the action of water.

To assess the water and O_2 impact on the HF in DB rocket propellant samples, a factorial analysis was performed, as illustrated in Figure S2. In the region where water and O_2 react with the propellant (a-b), the study found that increasing the concentration of water and O_2 causes an increase in HF. The same was observed in the region where propellant decomposition products react with the stabiliser (b-c). Pareto and normal probability distribution plots indicate that both O_2 and water contribute significantly to the HF, with O_2 being the most important factor. Furthermore, the interaction between the two factors was insignificant, as the p-value of the normal probability distribution was between 0.082 and 0.085 ($p < 0.05$ to be considered significant).

15214087, 0, Downloaded from https://onlinelibrary.wiley.com/doi/10.1002/prep.12070 by Cranfield University Kings, Wiley Online Library on [10/06/2025]. See the Terms and Conditions (https://onlinelibrary.wiley.com/terms-and-conditions) on Wiley Online Library for rules of use; OA articles are governed by the applicable Creative Commons License

4 | Conclusion

In this work, the effects of O_2 concentration and the presence of water on the decomposition of an EDB rocket propellant were assessed. The results show that both factors significantly influence the decomposition process. The results obtained from HFC indicate that as the water content increases, so does the HF. Similarly, an increase in O_2 concentration results in a higher HF.

The E_a was determined using the Friedman differential isoconversional method. The results show that in stages a-b (where the remaining O_2 interacts with the propellant) and b-c (where the propellant decomposes with the depletion of the main stabiliser), the E_a decreases as the water content increases, indicating that water catalyses the decomposition. Conversely, the E_a increases as the O_2 concentration decreases, suggesting a slower decomposition reaction. Further E_a evaluation by factorial design revealed that both water content and O_2 concentration negatively influence the E_a as they increase. However, O_2 is identified as the stronger influencing factor. Importantly, the results also show that there is no interaction between these two factors, allowing them to be studied independently.

In conclusion, this study highlights the importance of understanding the impact of O_2 concentration and water content on the decomposition of EDB rocket propellants for enhancing both safety and performance. By recognising water and O_2 as critical factors in the decomposition process, targeted strategies can be developed to mitigate their effects. Improving seals and/or integrating sensors to monitor oxygen and moisture within a rocket motor could significantly extend the shelf life of NC-based propellants, thereby increasing overall safety and reliability. This approach not only ensures the stability of the propellants over time but also contributes to the operational readiness and effectiveness of the rocket propulsion systems.

Conflicts of Interest

The authors declare no conflicts of interest.

Data Availability Statement

The data that support the findings of this study are available from the corresponding author upon reasonable request.

References

1. Office of Scientific Research and Development and National Defense Research Committee. Summary Technical Report of Division 3, NDRC. Volume 1, Rocket and Underwater Ordnance. (1946).

2. G. Evans and S. Gordon, "Considerations Concerning the Service Life, Handling and Storage of Double Base Solid Propellant Rocket Motors," in *8th Joint Propulsion Specialist Conference*. (1972), https://doi.org/10.2514/6.1972-1086.

3. A. Alm, "Studies on Reactions Between Nitrogen Dioxide and Diphenylamine Compounds," in *1st Symposium on the Chemical Problems Connected With the Stability of Explosives*. (1968).

4. R. Dobson, P. Folly, A. Sarbach, et al., "Making Progress Towards « Green » Propellants – Part III," *Propellants, Explosives, Pyrotechnics* 49 (2024): 1–11, https://doi.org/10.1002/prep.202300303.

5. A. Chin, D. S. Ellison, S. K. Poehlein, and M. K. Ahn, "Investigation of the Decomposition Mechanism and Thermal Stability of Nitrocellulose/Nitroglycerine Based Propellants by Electron Spin Resonance," *Propellants, Explosives, Pyrotechnics* 32 (2007): 117–126, https://doi.org/10.1002/prep.200700013.

6. B. Vogelsanger, "Chemical Stability, Compatibility and Shelf Life of Explosives," *Chimia* 58 (2004): 401, https://doi.org/10.2533/000942904777677740.

7. D. Trache and A. F. Tarchoun, "Analytical Methods for Stability Assessment of Nitrate Esters-Based Propellants," *Critical Reviews in Analytical Chemistry* 49 (2019): 415–438, https://doi.org/10.1080/10408347.2018.1540921.

8. M. A. Bohn and F. Volk, "Aging Behavior of Propellants Investigated by Heat Generation, Stabilizer Consumption, and Molar Mass Degradation," *Propellants, Explosives, Pyrotechnics* 17 (1992): 171–178, https://doi.org/10.1002/prep.19920170405.

9. C. O´Keeffe, I. Wallace, and P. P. Gill, "Effect of Humidity on the Real-Time, Low Temperature, Nitrocellulose Degradation by Chemiluminescence," in 7th International Nitrocellulose Symposium. (2016).

10. P. Guillaume, M. Rat, G. Pantel, and S. Wilker, "Heat Flow Calorimetry of Propellants—Effects of Sample Preparation and Measuring Conditions," *Propellants, Explosives, Pyrotechnics* 26 (2001): 51–57, https://doi.org/10.1002/1521-4087(200104)26:2⟨51.

11. R. Eerligh, W. P. C. de Klerk, and B. J. vd Meer, "Influence of Relative Humidity on Ageing of Propellants," in *11th Symposium on the Chemical Problems Connected With the Stability of Explosives*. (1998).

12. A. R. Jabalquinto, N. Mai, Y. Mohammed, and P. P. Gill, "Influence of Humidity on the Decomposition Process of Double Base Rocket Propellant," *Polymer Degradation and Stability* 218 (2023): 110546, https://doi.org/10.1016/j.polymdegradstab.2023.110546.

13. B. Lurie and B. Svetlov, "Chemistry and Kinetics of Nitrocellulose Thermal Decomposition," in *12th Symposium on the Chemical Problems Connected With the Stability of Explosives*. (2001), https://doi.org/10.1109/t-aiee.1950.5060110.

14. K. Katoh, L. Le, M. Aral, and M. Tamura, "Study on the Spontaneous Ignition of Cellulose Nitrate Effect of the Type of Storage Atmosphere (II)," *Science and Technology of Energetic Materials* 65 (2004): 77–81.

15. Z.-P. Li, J.-C. Jiang, A.-C. Huang, et al., "Thermal Hazard Evaluation on Spontaneous Combustion Characteristics of Nitrocellulose Solution Under Different Atmospheric Conditions," *Scientific Reports* 11 (2021): 24053, https://doi.org/10.1038/s41598-021-03579-z.

16. K. Katoh, L. Le, M. Kumasaki, Y. Wada, M. Arai, and M. Tamura, "Study on the Spontaneous Ignition Mechanism of Nitric Esters (II)," *Thermochimica Acta* 431 (2005): 168–172, https://doi.org/10.1016/j.tca.2005.01.067.

17. P. van de Mey and A. H. Heemskerk, "Stability of Nitrocellulose Propellants Assessed via Thermal Decomposition and Alteration of the Stabilizer Composition," *AGARD Conference Proceedings* 391 (1986): 9.

18. W. P. C. de Klerk, "Assessment of Stability of Propellants and Safe Lifetimes," *Propellants, Explosives, Pyrotechnics* 40 (2015): 388–393, https://doi.org/10.1002/prep.201500040.

19. L. D. Hansen, D. J. Eatough, E. A. Lewis, R. G. Bergstrom, D. Degraft-Johnson, and K. Cassidy-Thompson, "Shelf-life Prediction From Induction Period Calorimetric Measurements on Materials Undergoing Autocatalytic Decomposition," *Canadian Journal of Chemistry* 68 (1990): 2111–2114, https://doi.org/10.1139/v90-321.

20. C. Pichler, M. Schmid, R. Traxl, and R. Lackner, "Influence of Curing Temperature Dependent Microstructure on Early-age Concrete Strength Development," *Cement and Concrete Research* 102 (2017): 48–59, https://doi.org/10.1016/J.CEMCONRES.2017.08.022.

21. S. L. Zelinka, S. V. Glass, and E. Q. D. Lazarcik, "The Use of Isothermal Calorimetry to Measure Corrosion Rates of Metals in Contact

15214087, 0, Downloaded from https://onlinelibrary.wiley.com/doi/10.1002/prep.12070 by Cranfield University Kings, Wiley Online Library on [10/06/2025]. See the Terms and Conditions (https://onlinelibrary.wiley.com/terms-and-conditions) on Wiley Online Library for rules of use; OA articles are governed by the applicable Creative Commons License

With Preservative-treated Wood," *Thermochimica Acta* 727 (2023): 179575, https://doi.org/10.1016/j.tca.2023.179575.

22. W. Regenass, "The Development of Heat Flow Calorimetry as a Tool for Process Optimization and Process Safety," *Journal of Thermal Analysis* 49 (1997): 1661–1675, https://doi.org/10.1007/BF01983727.

23. T. Lindblom, "Reactions in Stabilizer and Between Stabilizer and Nitrocellulose in Propellants," *Propellants, Explosives, Pyrotechnics* 27 (2002): 197–208, https://doi.org/10.1002/1521-4087(200209)27:4⟨197::AID-PREP197⟩3.0.CO;2-W.

24. U. Ticmanis, S. Wilker, G. Pantel, et al., "Principles of a STANAG for the Estimation of the Chemical Stability of Propellants by Heat Flow Calorimetry," in *31st International Annual Conference of ICT*. (2000).

25. M. A. Bohn, "Principles of Ageing of Double Base Propellants and Its Assessment by Several Methods Following Propellant Properties," in *Proceedings of 49th International Annual Conference of ICT on 'Energetic Materials – Synthesis, Processing, Performance', June 26 to 29, 2018, Karlsruhe, Germany. ISSN 0722-4087. Fraunhofer-Institut fuer Chemische Technologie (ICT), D-76318 Pfinztal. Germany*. (2017) 9–11.

26. R. Tunnell, "Overview and Appraisal of Analytical Techniques for Aging of Solid Rocket Propellants," in *Chemical Rocket Propulsion*, eds. L. De Luca, T. Shimada, V. Sinditskii, and M. Calabro (Springer Aerospace Technology, 2017), 743–769, https://doi.org/10.1007/978-3-319-27748-6_31.

27. B. Roduit, P. Guillaume, S. Wilker, et al., Advanced Simulation of the Lifetime of Energetic Materials Based on HFC Signals. (2008).

28. S. Vyazovkin and N. Sbirrazzuoli, "Isoconversional Kinetic Analysis of Thermally Stimulated Processes in Polymers," *Macromolecular Rapid Communications* 27 (2006): 1515–1532, https://doi.org/10.1002/marc.200600404.

29. N. Sbirrazzuoli, "Model-free Isothermal and Nonisothermal Predictions Using Advanced Isoconversional Methods," *Thermochimica Acta* 697 (2021): 178855, https://doi.org/10.1016/j.tca.2020.178855.

30. B. Roduit, L. Xia, P. Folly, et al., "The Simulation of the Thermal Behavior of Energetic Materials Based on DSC and HFC Signals," *Journal of Thermal Analysis and Calorimetry* 93 (2008): 143–152, https://doi.org/10.1007/s10973-007-8864-3.

31. H. L. Friedman, "Kinetics of Thermal Degradation of Char-forming Plastics From Thermogravimetry. Application to a Phenolic Plastic," *Journal of Polymer Science: Polymer Symposia. Part C* 6 (1964): 183–195, https://doi.org/10.1002/polc.5070060121.

32. E. Torres-García, L. F. Ramírez-Verduzco, and J. Aburto, "Pyrolytic Degradation of Peanut Shell: Activation Energy Dependence on the Conversion," *Waste Management* 106 (2020): 203–212, https://doi.org/10.1016/j.wasman.2020.03.021.

33. B. Roduit, C. A. Luyet, M. Hartmann, et al., "Continuous Monitoring of Shelf Lives of Materials by Application of Data Loggers With Implemented Kinetic Parameters," *Molecules* 24 (2019): 2217, https://doi.org/10.3390/molecules24122217.

34. H.-W. Cui, J.-T. Jiu, T. Sugahara, et al., "Using the Friedman Method to Study the Thermal Degradation Kinetics of Photonically Cured Electrically Conductive Adhesives," *Journal of Thermal Analysis and Calorimetry* 119 (2015): 425–433, https://doi.org/10.1007/s10973-014-4195-3.

35. A. R. Jabalquinto, N. Mai, S. Belghiche, and P. P. Gill, "Modified Arrhenius Kinetics for Double Base Propellant Decomposition: Effect of Water," *Polymer Degradation and Stability* 227 (2024): 110846, https://doi.org/10.1016/j.polymdegradstab.2024.110846.

36. A. Dejeaifve, A. Sarbach, B. Roduit, P. Folly, and R. Dobson, "Making Progress Towards »Green« Propellants—Part II," *Propellants, Explosives, Pyrotechnics* 45 (2020): 1185–1193, https://doi.org/10.1002/prep.202000059.

37. B. Durakovic, "Design of Experiments Application, Concepts, Examples: State of the Art," *Periodicals of Engineering and Natural Sciences* 5 (2017): 421–439, https://doi.org/10.21533/pen.v5i3.145.

38. J. C. Spall, "Factorial Design for Efficient Experimentation," *IEEE Control Systems* 30 (2010): 38–53, https://doi.org/10.1109/MCS.2010.937677.

39. R. H. Myers, D. C. Montgomery, and C. M. Anderson-Cook, *Response Surface Methodology: Process and Product Optimization Using Designed Experiments* (Wiley, 2016).

40. D. C. Montgomery, "Using Fractional Factorial Designs for Robust Process Development," *Quality Engineering* 3 (1990): 193–205, https://doi.org/10.1080/08982119008918849.

Supporting Information

Additional supporting information can be found online in the Supporting Information section.

15214087, 0, Downloaded from https://onlinelibrary.wiley.com/doi/10.1002/prep.12070 by Cranfield University Kings, Wiley Online Library on [10/06/2025]. See the Terms and Conditions (https://onlinelibrary.wiley.com/terms-and-conditions) on Wiley Online Library for rules of use; OA articles are governed by the applicable Creative Commons License

https://dspace.org/

Factorial analysis of the influence of both water and oxygen on extruded double base rocket propellant decomposition

Romero Jabalquinto, Alonso; Mai, Nathalie; Heil, Moritz; Castedo, Guillermo Frades; Gill, Philip P.

2025-07
Wiley
https://doi.org/10.1002/prep.12070
Jabalquinto AR, Mai N, Heil M, et al., (2025) Factorial analysis of the influence of both water and oxygen on extruded double base rocket propellant decomposition. Propellants, Explosives, Pyrotechnics, Volume 50, Issue 7, July 2025, pp. 106-114

Downloaded from a DSpace repository. https://dspace.org/